HHS Public Access

Author manuscript

J Allergy Clin Immunol. Author manuscript; available in PMC 2020 October 01.

Published in final edited form as:

J Allergy Clin Immunol. 2019 October ; 144(4): 1058–1073.e3. doi:10.1016/j.jaci.2019.04.030.

IL-13-induced Intestinal secretory epithelial cell antigen passages are required for IgE-mediated food-induced anaphylaxis

Taeko K. Noah, PhD[a,b], **Kathryn A. Knoop, PhD**[e], **Keely G. McDonald**[e], **Jenny K. Gustafsson, PhD**[e], **Lisa Waggoner, Ms**[a], **Simone Vanoni, PhD**[a], **Matthew Batie**[c], **Kavisha Arora, PhD**[d], **Anjaparavanda Naren, PhD**[d], **Yui-Hsi Wang, PhD**[a], **Nicholas W. Lukacs, PhD**[a], **Ariel Munitz, PhD**[f], **Michael Helmrath, MD**[b], **Maxime M. Mahe, PhD**[b], **Rodney Newberry, MD**[e], **Simon P. Hogan, PhD**[a,b,*]

[a]Mary H Weiser Food Allergy Center, Department of Pathology, University of Michigan, Ann Arbor, MI

[b]Division of Allergy and Immunology, Department of Pediatrics, Cincinnati Children's Hospital Medical Center, Cincinnati, OH

[c]Division of Pediatric Surgery, Department of Pediatrics, Cincinnati Children's Hospital Medical Center, Cincinnati, OH

[d]Division of Clinical Engineering, Pulmonary Medicine, Department of Pediatrics, Cincinnati Children's Hospital Medical Center, Cincinnati, OH

[e]Division of Gastroenterology, Washington University School of Medicine St. Louis, MO

[f]Department of Clinical Microbiology and Immunology, Sackler School of Medicine, Tel Aviv University, Tel-Aviv, Israel

Abstract

Background: Food-induced anaphylaxis is an IgE-dependent immune response that may affect multi-organs and lead to life threatening complications. The processes by which food allergens cross the mucosal surface and are delivered to the sub-epithelial immune compartment to promote the clinical manifestations associated with food-triggered anaphylaxis are largely unexplored.

Objective: To define the processes involved in the translocation of food allergens across the mucosal epithelial surface to the subepithelial immune compartment in food-induced anaphylaxis (FIA).

[*]**Correspondence:** Simon P. Hogan, PhD, Mary H Weiser Food Allergy Center, Department of Pathology, University of Michigan 5063-BSRB 109 Zina Pitcher Place Ann Arbor, MI 48109-2200, sihogan@med.umich.edu. Phone: 734-647-9923; Fax: 734-615-2331.

Disclosures: Other authors have declared that they have no conflict of interest.

Methods: 2 photon (2P) confocal and immunofluorescence microscopy was employed to visualize and trace food allergen passage in a murine model of FIA. Human colon cancer cell line, RNA silencing and pharmacological approaches were used to identify the molecular regulation of intestinal epithelial allergen uptake and translocation. Human intestinal organoid transplants were employed to demonstrate the conservation of these molecular processes in human tissues.

Results: Food allergens are sampled by small intestine (SI) epithelial secretory cells (termed SAPs) that are localized to the SI villus and crypt region. SAPs channel food allergens to lamina propria mucosal mast cells via IL-13-CD38-cADPR-dependent process. Blockade of CD38/cADPR-dependent SAP antigen passaging in food allergic mice inhibited the induction of clinical manifestations of FIA. IL-13-CD38-cADPR-dependent SAP sampling of food allergens was conserved in human intestinal organoids.

Conclusion: We identify that SAPs are a mechanism by which food allergens are channeled across the SI epithelium, mediated by IL-13/CD38/cADPR pathway and regulate the onset of food-induced anaphylactic reactions and are conserved in human intestine.

Graphical Abstract

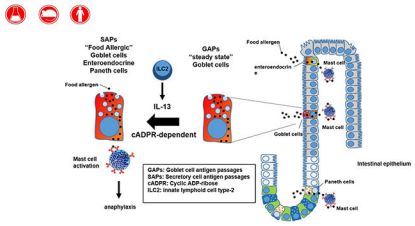

One sentence Summary:

Antigen passages across the gastrointestinal epithelium induces food allergic reactions

Capsule Summary:

Food allergens translocate across the gastrointestinal intestinal epithelium to induce a food allergic reaction through Secretory antigen passages (SAPs) via IL-13-Type II IL-4R-CD38/cADPR-dependent pathway.

Keywords

food allergy; antigen passages; intestinal epithelium; mast cells; anaphylaxis; secretory cells

Introduction

Anaphylaxis is a severe, life-threatening allergic reaction that affects both children and adults and male and female subjects in the United States [1]. Food avoidance is the primary recommended treatment strategy for food-induced anaphylaxis and hospitalization rates for children in the United States have more than doubled from 2000 to 2009 [2]

Clinical and experimental analyses have identified that crosslinking of the food allergen:IgE complex to FcεR on mast cells (MCs) and basophils drives the secretion of autacoid

mediators that act on target organs (gastrointestinal, cutaneous, respiratory, cardiovascular) and incite the clinical manifestations of food-induced anaphylaxis [3–11]. Though the immune pathways involved in orchestrating the pro-allergic inflammatory repertoire and downstream MC effector response have been extensively delineated [12, 13], little is known about how food allergens cross the mucosal barrier and stimulate an IgE-MC activation and promotion of the clinical manifestations of disease.

Translocation of oral antigens across the SI epithelium is thought to occur via; micro fold (M) cell-mediated transcytosis [14–16], transepithelial dendrites (TEDs) [17], Goblet cell antigen passages (GAPs) [18] and paracellular leak [19]. In healthy individuals, M cell-mediated transcytosis and GAP-mediated transcellular transport seem to be the main route of luminal antigen sampling [18]. However, the molecular basis by which food allergens translocate across the allergic intestinal epithelium and induce a food-induced IgE-mediated reaction remains unclear.

Herein, we demonstrate that secretory epithelial cells in the small intestine (SI) of food allergic mice act as conduits to permit food allergen transport across the SI epithelium to MCs. We show that the SI intestinal secretory epithelial cell antigen passages (SAPs) comprise villus and cryptic goblet cells (GCs), enteroendocrine cells, and Paneth cells; are induced by IL-13 in a CD38/cADPR-dependent manner; and are conserved in humans. Our *in vivo* analyses reveal that SAPs are integral for the initial translocation of food allergens across the SI epithelium to underlying mast cells that lead to the induction of a food-induced anaphylactic reaction.

Results

Food allergens translocate across small intestine via goblet cells in villi.

To examine how food allergens translocate across a mucosal surface such as the SI, fluorescently labelled food allergens (cow's milk and egg) were intraluminally injected into the SI of naïve wild type BALB/c mice and monitored for localization using fluorescence microscopy. At steady state, we observed a thin layer of food allergen covering the apical surface of the epithelium indicating SI epithelial cell exposure to the allergens (Fig 1A). We observed occasional transepithelial columns (data not shown) that resembled the recently identified carbachol (CCh)-induced goblet cell antigen passages (GAPs) which act as conduits for the delivery of SI luminal antigens to immune cells [18]. To determine if the transepithelial columns were GAPs, fluorescently labelled food allergens were intraluminally administered to naïve wild type BALB/c mice treated with CCh. We show that the frequency of food allergen positive SI transepithelial columns were increased following CCh treatment (Fig 1A, white arrows) and localized within $MUC2^+$ cells indicating that clinically relevant food allergens in naïve mice are acquired by GAPs (Fig 1B, green arrows).

Egg antigen ovalbumin (OVA) is a model food allergen commonly used to induce food allergic reactions in mice. To monitor the localization of the food allergen OVA and the model imaging protein 10 kDa lysine fixable dextran conjugated with rhodamine (Rh-Dex) in the SI, we intraluminally coadministered Alexa Fluor 647-labelled OVA and Rh-Dex to

naïve wild type BALB/c mice. Similar to the clinically relevant food allergens, OVA and the imaging protein Rh-Dex localized to $MUC2^+$ transepithelial columns (Fig 1C). The colocalization of Rh-Dex and OVA within $MUC2^+$ intestinal epithelial cells in the SI both indicates shared SI epithelial uptake processes between clinically relevant food allergens, model food antigens, and model imaging proteins.

Food Allergen translocation across SI epithelium is enhanced in food allergic mice.

We next examined food allergen passage in the SI of food allergic mice. To do this, we utilized a murine model of food allergy [20] that we developed that involves repeated intra-gastric administration of egg antigen (OVA) to OVA-sensitized BALB/c mice that induces an acute IgE-MC–dependent anaphylactic reaction [20–22] (Fig 1D) as evidenced by a hypothermic response within 30 minutes of antigen exposure (Supplementary Figure S1A). In order to visualize the spatial and temporal elements of food allergen uptake in the SI of food allergic mice, we utilized intravital live imaging with 2P microscopy (Supplementary Video 1–3). In naïve mice, the imaging antigen (Rh-Dex) was restricted to the luminal space. We observed the occasional transpeithelial column formation and SI epithelial antigen uptake (indicated by colocalization of Rh-Dex and DAPI). Furthermore, the lamina propria region beneath DAPI positive SI epithelium remained free of Rh-Dex (Supplementary Video 1). Similarly, examination of the SI of food allergic mice prior to the allergen exposure revealed infrequent SI transepithelial columns and the lamina propria was mostly free of Rh-Dex (Supplementary Video 2). Exposure of the SI of food allergic mice to food allergen rapidly enhanced antigen uptake within minutes (Supplementary Video 3). Furthermore, we observed accumulation of Rh-Dex within the lamina propria following SI exposure to food allergen indicating translocation of food allergens across the intestinal epithelium (Supplementary Video 3). Immunofluorescence analyses of the SI of food allergic BALB/c WT mice following food challenge (Day 28, Fig 1D) revealed localization of OVA antigen to villus transepithelial columns (Fig. 1F). Similarly to naïve wild type mice, fluorescently-labelled OVA and Rh-Dex colocalized to $MUC2^+$ GCs in the food allergic mouse SI (Fig 1C and F). Consistent with the live imaging analyses, quantification of the number of GAPs revealed a significantly greater number of antigen passages in the SI of food allergic mice than that observed in naïve WT BALB/c at steady state and following CCh stimulation (Fig 1G). These studies suggest increased luminal antigen uptake in the SI under the allergic condition.

Allergen translocation in food allergic SI involves secretory cells in villi and crypts.

Repeated i.g. administration of OVA to OVA-sensitized BALB/c leads to increased SI GC levels (Fig 1E, alcian $blue^+$ cells). Given that GAP formation is tightly associated with goblet cell number [18], we hypothesized that the increase in frequency of OVA^+ cells was a consequence of increased number of GAPs. Microscopic examination of the SI villus-crypt unit of the allergic mouse indeed revealed increased number of antigen-positive GCs (Fig 1F and J), however we also observed the presence of previously undescribed $MUC2^-$ $Rh\text{-}Dex^+$ cells in the SI villus (Fig. 1I; green arrow) and of antigen passages within the crypts (Fig. 1H). Immunofluorescence analyses of the villus revealed the $MUC2^-Rh\text{-}Dex^+$ cells as enteroendocrine cells (chromogranin A [$ChrA^+$]), whereas the crypt comprised both enteroendocrine ($ChrA^+Rh^-Dex^+$) and Paneth cells (Paneth cell marker metalloproteinase 7

[MMP7]$^{+}$Rh^{-}Dex^{+} cells), indicating the participation of enteroendocrine and Paneth cells in the uptake of food antigens (Fig. 11, red arrows). Tuft cell marker DCLK1 (Supplementary Fig. S1B) did not colocalize with Rh-Dex^{+}, indicating that tuft cells do not sample SI food antigens in food allergic mice. These data indicate that under food allergic conditions, multiple intestinal secretory cell lineages within the SI acquire and channel food antigens from the apical to basolateral side, which we defined as SI intestinal secretory epithelial cell antigen passages (SAPs). Quantification of Rh-Dex^{+} cells revealed a higher frequency of villus and the presence of crypt Antigen Passages (v- and c-AP) in the SI of food allergic mice, and while GCs were the predominant intestinal secretory cell involved in antigen uptake (~65%), endoendocrine and paneth cells can also uptake food allergens (Fig. 1J). Examination for SAPs in other GI compartments revealed the presence of Rh-Dex^{+} surface mucous cells within the stomach, however we observed no Rh-Dex^{+} staining in the gastric pits within the mucous neck, parietal or chief cells (Supplementary Fig. S1C). Rh-Dex^{+} cells were observed within the ileum villus colocalizing with MUC2^{+} and CgA^{+} indicating GC and enteroendocrine cells forming antigen passages, however we did not observe evidence of MMP7^{+} (Paneth cells) forming SAPs at the bottom of the crypts (Supplemental Fig. 1D). Consistent with our recent findings [23] we also observed the occasional MUC2^{+} cells forming antigen passages within the colon, however this was rare (Supplementary Fig. 1E).

Antigen translocation via SAPs to underlying mast cells

The onset of food-induced anaphylaxis in mice requires intestinal mastocytosis and mucosal MC activation mediated by the food antigen:IgE complex [20, 22]. From the rapid onset of symptoms of an anaphylactic reaction after allergen consumption (5-10 min, Supplementary Figure 1A), we hypothesized that SAPs must directly interact with mucosal MCs. Mucosal MCs within the SI of food allergic mice are predominantly localized to the basolateral membrane of the villus and crypt secretory epithelial cells or within the intraepithelial region positioned midway along the intestinal epithelial cells lateral membrane (Fig. 2A, Allergic). Histological analysis of the SI of food allergic mice prior to food antigen exposure (Day 28) revealed the presence of mucosal MCPT-1^{+} MCs in close proximity to villus GCs (Fig. 2B, red arrows for MCs and green arrows for GCs) and localized at the basal membrane of crypt Paneth cells (Fig. 2C, red arrow). Upon allergen exposure, we observed enhanced SAP formation, Rh-Dex localization within LP and colocalization of Rh-Dex^{+} and MCPT-1^{+} MCs in villus and crypts (Fig. 2D & E red arrows and Supplementary Video 6). SI MC specific antigen uptake was confirmed by flow cytometry of SI LP single cell suspensions which revealed a significant increase in the number of Rh-Dex^{+} FcϵR1^{+} C-Kit^{+} ST2^{high} MC's in food allergic mice following OVA^{+} Rh-Dex exposure (Fig. 2F–G). These studies suggest that SI SAPs rapidly channel food antigens to mucosal MCs in food allergic mice and this process is enhanced by food allergen exposure.

IL-13 is sufficient to drive SAP formation and secretory cells are required for IL-13 driven antigen passages

The pro-allergic cytokine IL-13 plays a major role for inducing the clinical manifestations of food-induced anaphylaxis [24] and has been shown to modulate intestinal secretory epithelial cell lineage function including GC hyperplasia (Fig 3A) [25]. Thus, we hypothesized that IL-13 can stimulate SI SAPs. Indeed, analyses of intestinal iIL-13Tg mice revealed that

ectopic expression of IL-13 in the SI epithelium is sufficient to induce SAPs (Fig. 3B, green and red arrows). Cross-sectional analysis of SI indicates that GC and GAP abundance was significantly higher in iIL-13Tg than WT (BALB/c) mice (naive, 0.40 ± 0.03 vs iIL-13Tg, 2.60 ± 0.41; GAPs/villus, p-value < 0.05) (Fig. 3C). In addition to the increased GAP formation in iIL-13Tg villi, we identified $MUC2^{-}$ antigen passages in the SI villus and crypts of iIL-13Tg mice similarly to food allergic mice (Fig. 3B–E), indicating that SI overexpression of IL-13 is sufficient to mimic the SI SAP phenotype observed in food allergic mice.

To determine the requirement of SI secretory epithelial cells in SAP formation driven by IL-13, we used *Atohl* mutant mice (*Atoh1*-MT), in which all cells of the secretory lineage are deleted from the intestinal epithelium after Tamoxifen treatment[26]. Treatment of *Atoh1*-MT mice with Tamoxifen led to a loss of secretory lineage cells in the SI (Fig. 3F). Intraluminal administration of Rh-Dex to *Atoh1*-WT treated with IL-13 revealed SAP formation in the villus and crypts (Fig. 3G). Tamoxifen treatment alone of *Atoh1*-WT mice did not drive SAP formation (Supplementary Fig. 1F). In contrast to Atoh1-WT mice, we observed no evidence of SI villus or crypt transpeithelial columns in *Atoh1*-MT mice (Fig. 3G), indicating that intestinal epithelial cells of the secretory lineage are required for IL-13 driven luminal antigen passage formation.

IL-13 drives SAP formation through a STAT6-independent PI3K-CD38-cADPR – dependent process

To study the signaling cascade involved in IL-13–induced SAP formation, we used LS174T, a mucinous colon cancer cell line [27] We show that exposure of LS174T cells to IL-13 induced antigen uptake (Supplementary Fig. S2A, Rh-Dex^{+} cells) that was associated with the type II IL-4 receptor–dependent STAT6/PI3K activation, as evidenced by phosphorylation of STAT6 and AKT^{Ser473} (Supplementary Fig. S2B–E). Genetic abrogation of STAT6 in LS174T cells failed to reduce IL-13–mediated antigen uptake, indicating that IL-13 induced SAPs independent of STAT6 signaling (Supplementary Fig. S2A and G). In contrast, pharmacologically inhibiting the PI3K pathway (LY294002, a specific PI3K inhibitor) inhibited IL-13–induced antigen uptake in a dose-dependent manner (Fig. 4A and B, IL-13 0.03 ± 0.01 vs. IL-13^{+} LY294002 1 μM 0.01 ± 0.01 or 10 μM 0 ± 0.00 % Rh-Dex^{+} cells, mean ± SEM, *p < 0.05). Given that IL-13–induced PI3K activation drives intracellular calcium ($[Ca^{2+}]_i$) release via a CD38/cADPR-dependent mechanism [28] and that $[Ca^{2+}]_i$ release is strongly associated with secretatogue activity [29], we examined the necessity of the CD38/cADPR pathway in IL-13–induced antigen uptake. Inhibiting the CD38/cADPR pathway with the cADPR antagonist 8-Br cADPR abrogated IL-13–induced $[Ca^{2+}]_i$ release in LS174T cells in a dose-dependent manner (Fig. 4C and Supplementary Fig S2F). Abrogation of IL-13–induced $[Ca^{2+}]_i$ in LS174T cells inhibited SAP formation (Fig.4 D and E, IL-13 0.11 ± 0.03 vs. 8 Br cADPR 5 μM 0.02 ± 0.02 or 10 μM 0.01 ± 0.01 % Rho-Dex^{+} cells, mean ± SEM, p < 0.05). Consistent with our *in vitro* analyses, treating iIL-13Tg mice with 8 Br-cADPR suppressed SAP formation in the SI (Fig. 4F and G). Treating iIL-13Tg mice with the M4AchR antagonist Tropicamide did not affect the frequency of SAPs (Fig. 4F and G), indicating that IL-13–driven SAP formation is dependent on the

CD38/cADPR pathway and independent of the M4AchR pathway. Collectively, these data support that IL-13 induces SAPs via a CD38/cADPR pathway through $[Ca^{2+}]_i$ release.

IL-13 directly drives antigen passage formation on intestinal secretory cells.

To determine the requirement of intestinal epithelial secretory cell IL-13 signaling on SAP formation and food-induced anaphylaxis we crossed Atoh1^{Cre*GR} IL4Rα$^{F/F}$ mice to IL9Tg mice in which IL-9 was ectopically expressed in the SI epithelium and promotes mastocytosis in the SI [30] We show that administration of the competitive progesterone receptor antagonist RU486 deleted IL-4Rα from Atoh1^{+} cell lineages (Fig. 5 A&B; white arrow). Deletion of IL-4Rα from secretory cells did not cause any obvious morphological changes in SI at steady state (Fig 5C). Genetic deletion of IL-4Rα from secretory intestinal epithelial cell lineages inhibited IL-13-induced SAP formation (Fig. 5B & D) indicating involvement of secretory cells in antigen passage formation and dependency on intestinal epithelial IL-13 signaling through IL-4Rα for the antigen passage formation. Administration of RU486, anti-TNP IgE and IL-13 to IL9Tg Atoh1^{WT}IL4Ra$^{F/F}$ mice (IL-4Rα^{WT}; IL9Tg) and subsequent oral challenge with antigen (TNP-OVA) induced a shock response (Fig. 5E). In contrast, injection of anti-TNP-IgE and IL-13 and subsequent TNP-OVA challenge of IL-9Tg Atoh11^{Cre*GR}IL4Rα$^{fl/fl}$ mice (IL-4Rα$^{\Delta secretory}$; IL9Tg) that received RU486 did not develop shock response (Fig. 5E). These studies indicate that intestinal epithelial secretory cell intrinsic IL-4Rα pathway is required for IL-13-induced SAP formation and induction of passive IgE-mediated oral-antigen anaphylaxis.

Blockade of IL-13-IL-13Rα1 signaling reduces antigen passages and protects against food-induced anaphylactic shock.

The demonstration that IL-13-induced SAPs was dependent on epithelial secretory cell intrinsic IL-4Rα signaling suggests that IL-13 is acting through the Type II IL-4R (IL-4Rα / IL-13Rα1)[31]. Notably, both IL-4 and IL-13 can signal through the Type II IL-4R (IL-4Rα / IL-13Rα1)[32, 33]. To test whether IL-4 is sufficient to drive SAPs, WT BALB/c mice received rmIL-4 (65ng / 200μl i.v.) and twenty-four hours later we examined evidence of SI SAPs. We show that exposure of rmIL-4 was sufficient to significantly upregulate MHC class II expression on B cells confirming IL-4 biological activity (Supplementary Figure S3), however, IL-4 treatment was not sufficient to upregulate the frequency of SI antigen passages (Supplementary Figure S3) revealing that SAP formation is a IL-13-specific effect. To determine the requirement of IL-13 driven SAPs in the induction of a food-induced anaphylactic reaction, BALB/c mice that had previously demonstrated a history of reactivity to foods (5th challenge) received repeated administration of anti-IL-13Rα1 monoclonal antibody[34] (Fig. 5F) during the sixth and 7th oral OVA challenge and evidence of a food-induced anaphylactic reaction and SI SAPs were examined. We show that administration of anti-IL-13Rα1 monoclonal antibody to food allergic mice abrogated MUC2^{+} GCs (Fig. 5G) and reduced the frequency of SI SAPs (Fig. 5G and H) as compared with isotype control-treated mice. Notably, reduced frequency of SI SAPs was associated with a significant reduction food-induced anaphylactic symptoms (shock and diarrhea) (Figure 5H) and that this was associated with reduced levels of MC activation (Fig 5H). Spearman's rank coefficient correlation analysis revealed a significant negative correlation between frequency of SAPs and shock response (Δ temperature change ($r = -0.9649$, $p < 0.005$), indicating a

relationship between SAPs and severity of oral antigen-induced anaphylaxis. Collectively, these studies indicate that IL-13-induced SI SAPs play a significant role in passage of luminal food allergens across the SI epithelium and severity of oral antigen-induced anaphylaxis.

Pharmacological blockade of IL-13/CD38-cADPR-driven SAP formation protects mice from the onset of food-induced anaphylactic shock.

To determine the requirement of IL-13/CD38-cADPR-pathway driven SAPs in the induction of a food-induced anaphylactic reaction, BALB/c mice that had previously demonstrated a history of reactivity to foods were administered CCh/M4AchR inhibitor (Tropicamide) or IL-13/CD38-cADPR inhibitor (8-Br cADPR) and challenged with OVA (Fig. 6A). Tropicamide treatment did not affect villus SAP formation or food antigen passage in allergic mice or Rh-Dex$^+$ mast cell number (Fig. 6B–D and Supplementary Video S3 and S4), and the mice proceeded to develop food-induced anaphylaxis as evidenced by hypovolemic shock and MC activation (Fig. 6 E and F). In contrast, pretreating food allergic mice with 8-Br cAPDR significantly decreased villus SAP formation and Rh-Dex$^+$ mast cells (Fig. 6B–D) and abrogated MC activation and onset of food-induced anaphylactic symptoms (Fig. 6 E and F and Supplementary Video S3 and S5). 8-Br cADPR or Tropicamide treatment did not significantly impact MC degranulation capacity as MC activation induced by EM95 (anti-IgE antibody) treatment and shock response (Fig 6G). Furthermore, 8-Br cADPR or Tropicamide treatment did not impact vascular endothelial function as histamine-induced shock response was equivalent to control treated mice (data not shown). These data indicate that the loss of symptoms of food-induced anaphylaxis was not a result of 8-Br cADPR–mediated inhibition of downstream MC activity or histamine-driven shock response.

IL-13 driven SAP formation through the PI3K-CD38-cADPR pathway is conserved in human intestine

To determine whether IL-13–induced SAPs were conserved in human SI, we examined for the presence of SI SAPs in human intestinal organoids (HIOs) generated from pluripotent stem cells [35] that were transplanted onto the mesentery of NSG mice (tHIOs) (Fig. 7A). Intestinal secretory cells in tHIOs are morphologically and functionally mature and resemble SI epithelium (Fig. 7B). Intraluminal administration of fluorescently labelled milk to the tHIO of CCh-treated mice induced the formation of transepithelial food antigen (milk) columns in tHIOs (Fig. 7C; white arrows left panel). The milk$^+$Rh-Dex$^+$ tHIOs were restricted to MUC2$^+$ cells and sensitive to M4-AchR inhibition, supporting the concept of CCh-dependent, GC-restricted antigen passages at steady state (Fig. 7C, E and F). Administration of IL-13 to tHIOs induced both MUC2$^+$Rh-Dex$^+$ and MUC2$^-$Rh-Dex$^+$ phenotypes (Fig. 7D, white arrows) in the villus and crypts of tHIOs, which was abrogated by 8-Br cADPR treatment, indicating that IL-13–induced SAP formation in both the villus and crypts is conserved in humans (Fig.7 G red and green arrows and H). These studies reveal that the IL-13/CD38/cADPR-dependent SAPs are conserved within human intestinal tissue.

Discussion:

Herein, we demonstrate that food allergens in the SI of food allergic mice are channeled across the intestinal epithelium via secretory intestinal epithelial cells which we have termed SAPs. We show that SAP formation and food allergen passage is rapidly induced by food allergens, and permitting the passage of food allergens to underlying mucosal mast cells. We show that the pro-type 2 cytokine IL-13 induces SAPs via a STAT6-independent and CD38-cADPR-sensitive pathway and requires SI intestinal epithelial expression of IL-4Rα. Blockade of this process abrogated food allergen passage across the SI epithelium and diminished the induction of a food allergic reaction in mice. Finally, we show that antigen passages and IL-13-induced CD38-cADPR-sensitive SAPs are conserved in human tissue.

Previous studies have revealed that SI steady state antigen passages are restricted to the SI villus and GCs, primarily driven by an acetylcholine (Ach) muscarinic M4 type receptor (M4AchR)-dependent manner [23]; unresponsive to commensal microbes, however sensitive to EGF-mediated inhibition [23]. We show that in food allergic mice the luminal antigen sampling epithelial repertoire in the SI is altered, consisting of additional SI secretory epithelial populations including enteroendocrine and paneth cells, is unresponsive to M4AchR-dependent signaling and dependent on IL-13-induced CD38/cyclic adenosine diphosphate ribose (cADPR) signaling. The participation of additional secretory intestinal epithelial cells in antigen passaging during the food allergic condition can be explained by activation through allergic inflammatory pathways such as IL-13. However, the observation of GC participation in antigen passaging at steady state and during the allergic condition and a shift from M4AchR-induced to IL-13-induced M4AchR-unresponsive phenotype suggests a more complex mechanism for GCs. It is possible that GCs involved in antigen passages at steady state are modified by IL-13 and become unresponsive to M4AchR-dependent signaling. Alternatively, different GC subsets may contribute to M4AchR-induced steady state vs IL-13-induced allergic antigen passages. We have previously reported that not all GCs are involved in steady state antigen passages [18], so it is possible that different GC subsets are involved in antigen passaging during the allergic condition versus those involved in antigen passaging at steady state. Differential involvement of GC subsets in antigen passage formation at steady state and under allergic conditions may explain the differential interactions with hematopoietic cells such as DCs and MCs.

Our data supports the concept that the alteration in antigen sampling epithelial repertoire in the SI in food allergic mice is directly mediated by IL-13. We showed that 1) ectopic transgenic expression of IL-13 in the SI was sufficient to drive SAP formation; 2) that SAP formation required intestinal secretory cell IL-4Rα expression and 3) that administration of hIL-13 to NSG mice (lack the adaptive immune cells) was sufficient to induce SAPs in *h*HIOs. IL-13 has previously been reported to stimulate GC hyperplasia and mucus secretion, Paneth cell degranulation and entoerendocrine cell function [36–38]. The present study identifies a novel role for IL-13 in the regulation of intestinal secretory epithelial cell function associated with food antigen translocation and induction of food allergic reactions. The cellular source of IL-13 for SAP induction in the food allergic SI is currently not fully delineated. ILC2 may be the cellular source of IL-13 since SI ILC2s are a major source of

IL-13 in food allergic mice and that the onset of food allergy required IL-13$^+$ produced by ILC2s [24].

We have previously demonstrated that genetic or pharmacological deletion of GAPs was associated with a loss of antigen delivery to SI LP DCs suggesting that SI GAPs are the primary pathway for delivery of SI luminal antigen to the adaptive immune compartment in the basal state [18]. In the present study we show that SAPs facilitate food allergen passage to SI MCs indicating that multiple hematopoietic cell populations can acquire antigen through intestinal epithelial passages. Fluorescent microscopy analysis revealed that in food allergic mice, mucosal MCs appear to predominantly localize to the basolateral membrane of SAPs. Demonstration that food antigen exposure led to the rapid channeling of antigen through the SAPs and acquisition by MCs immediately beneath the lateral membrane of the SAPs makes it tempting to speculate that MCs are selectively recruited to this location to sense luminal antigens channeled by SAPs [39] This may explain the concentrated amplification of mucosal MCs within the subepithelial region that is dependent on IL-9-driven SI mastocytosis required in the induction of food-induced reaction in mice [30].

In vitro analyses revealed that IL-13 stimulation of LS174T cells led to heightened intracellular [Ca^{2+}] responses and antigen passages that was STAT6-independent and inhibited by 8-bromo-cADPR. Previous studies have reported that IL-13 stimulation of human airway smooth muscle cells leads to increased CD38 expression and ADP-ribosyl cyclase activity that was associated with heightened [Ca^{2+}]$_i$ activity and responsive to 8-bromo-cADPR [28, 40]. IL-13 activation of the Type II IL-4 receptor pathway (IL-4Rα-IL-13Rα1) leads to IL-4Rα-bound IRS-2 phosphorylation and activation of the PI3K-Akt pathway stimulating [Ca^{2+}]i activity [31, 41]. Collectively these studies establish a link between GC secretion by compound exocytosis, [Ca^{2+}]$_i$ activity and SAP formation.

The precise mechanism by which food allergens stimulate SAP formation and passage of antigens to mucosal MCs is currently unknown. We demonstrate that food allergic mice possess SAPs, and that food allergen exposure rapidly enhances SAP formation. Berin and colleagues have previously reported that oral antigen exposure of rat SI led to rapid antigen uptake into vesicles of epithelial cells of the SI [42] SI epithelial antigen uptake was linked with the expression of the low affinity IgE receptor (FcεRII) on SI intestinal epithelial cells and neutralization of FcεRII function inhibited luminal antigen uptake [43] It is not clear if FcεRII or IgE are involved in SAP formation and antigen translocation. However, given that administration of hIL-13 to NSG mice is sufficient to stimulate SAPs in tHIO's suggests that additional mechanisms beyond adaptive immunity recognition pathways are involved in the process.

Previously we have reported that GAPs within the GI tract channel luminal high-molecular-weight substances to LP-APCs such as CD11c$^+$ dendritic cells and drive antigen-specific T-cell responses[18, 44] These studies raise the concept that GCs and GAPs may contribute to the delivery of luminal food antigens to the immune compartment for the induction of T-cell responses outside of the organized lymphoid tissues and regulate oral tolerance vs food sensitization. The role of GAPs in inducing tolerance to dietary antigens in the steady state is yet to be explored, however experimental evidence demonstrating that dysregulation of

GAP activity promotes inflammatory T cell responses to dietary antigens [45] and our observations that certain conditions such as elevated Type-2 cytokines, can alter SI epithelial antigen passage patterning (GAPs vs SAPs) and promote channeling of antigens to additional cell populations such as mast cells leads one to speculate that dysregulation of antigen passages may lead to altered responsiveness to dietary antigens (oral tolerance vs food sensitization). Consistent with this concept, modulation of GAP patterning of the GI tract during preweaning stage in mice can alter mice susceptibility to colitis [46].

In summary, we identify SI SAPs in food allergic mice and these processes are enhanced by the allergen exposure to rapidly channel food allergens across the SI epithelium. We show that both mouse and human SI SAPs are induced by IL-13 in a CD38/cADPR-dependent manner and are required for passage of food allergens across the SI epithelium and induction of a food-induced anaphylactic reaction. These studies reveal the ability of the pro-allergic cytokine IL-13 to remodel the SI antigen uptake architecture under conditions of food allergy, which enables the routing of luminal antigens to intestinal MCs and induction of food-induced anaphylactic reactions. Given that Th2 cytokine responses are associated with other afflictions (e.g., helminthic infestation) and allergic diseases (e.g., allergic rhinitis, asthma), SAPs may extend to other Th2-driven conditions. Indeed, SAPs may be a generalizable hallmark of IL-13–induced immune responses at mucosal surfaces, and strategies to circumvent SAPs may have therapeutic potential for many Th2-associated conditions.

Material and Methods

Mice

Six- to ten-week old BALB/c (wildtype, WT), intestinal IL-13 transgenic (iIL-13Tg)[30], VilCre^{ERT2} Atoh1$^{fl/fl}$ mice [47] were used for GAP/SAP formation analysis and oral antigen–induced anaphylaxis studies [20]. Atoh1^{cre*GR} mice [48] were purchased from the Jackson Laboratory and crossed to IL-4Rα$^{fl/fl}$[49] then to IL-9Tg [30] Six-to ten-week old IL-9Tg Atoh1^{cre*PR} IL-4Rα$^{fl/fl}$ (IL-4Rα$^{\Delta secretory}$) and IL-9Tg Atoh1^{WT} IL-4Rα$^{fl/fl}$(IL-4Rα^{WT}) mice were used for SAP formation and induction of passive IgE-mediated oral-antigen anaphylaxis. Six-eight-week old immune-deficient NOD-SCID IL-2Rγ^{null} (NSG) mice obtained from the Comprehensive Mouse and Cancer Core Facility at Cincinnati Children's Medical Center (CCHMC) were used for HIO transplantation experiments as previously described [35]. All animals were cared and handled as described in the protocols approved by the Animal Care and Use Committee at CCHMC.

Reagents

Food antigens [cow's milk (Organic Valley Family of farms), and egg (Jay Robb Enterprises Inc) and ovalbumin) were conjugated to Alexa Fluor 647 dye as described by the manufacturer (ThermoFisher Scientific). The model antigens and inhibitors used were as follows: dextran, tetramethylrhodamine, 10,000 MW, lysine fixable and diamidino-2-phenylindole (DAPI) (ThermoFisher Scientific); 8-Br cADPR (Sigma); Tropicamide (SantaCruz); LY294002 (Cell signaling). The reagents used are as follows: Fluo4 AM and Imject Alum Adjuvant (ThermoFisher Scientific); RU486, polybrene, tamoxifen, carbachol,

histamine and ovalbumin (Sigma Aldrich), human and mouse IL-13 (PeproTech), and mouse anti-IgE antibody, clone EM-95 (provided by Fred D. Finkelman at CCHMC). Antibodies that we used are as follows: Chromogranin A (Immunostar), MMP7 (R&D systems), mouse MCPT-1 (eBioscience), MUC2, STAT6, IL-4Rα, phospho-STAT6 (SantaCruz), phospho-AKT (Ser473) and phospho-AKT (Thr308) (#9275, Cell Signaling), actin (A2066, Sigma), DCLK1 and anti-GFP (Abcam), PerCP-Cy5.5 conjugated CD45R/B220, CD8, Ly-6G/Ly-6C, CD11c, and CD3e, PE/Cy7 conjugated ckit, biotin conjugated ST2 (BioLegend), streptavidin conjugated APC-Cy7 (BD Pharmigen), and APC conjugated FcεR (BioLegend), Donkey anti-mouse, -rat, -rabbit & -goat conjugated to Alexa Fluor-488 or −647 (Invitrogen).

Immunofluorescence, histological analysis & microscopy

Harvested tissues were fixed in 4% paraformaldehyde in PBS, then processed and embedded either in O.C.T. compound or paraffin. Cross sections of tissues were stained with the antibodies indicated and nucleus were visualized with DAPI. All immunofluorescence imaging was performed using Zeiss Apotome Wide Field Microscope equipped with 10×/0.3 NA, 20×/0.5 NA, 40×/0.75 NA, 63×/1.4 NA-oil immersion objectives in the wide-field mode. Z-stack images were reconstructed into 3D using Imaris software and 2D images were generated by applying extended focus to z-stack images. Photomicrograph images were taken with Olympus BX51 equipped with a 20×/0.5 NA objective using cellSens software.

Intravital 2P microscopy

Imaging of murine GI segments was performed as previously described [18]. Briefly, intact GI tissue was surgically extracted from the abdominal cavity and placed on a heated plate mounted on the mouse abdomen to minimize the tissue movement from mouse breathing during imaging. The model fluorescent antigens (Rh-Dex) were injected intraluminally 15 min prior to imaging. With the naïve mice, the SI segment was imaged following PBS exposure. All imaging was performed using a A1R Multiphoton Upright Confocal Microscope equipped with resonant and galvanometric dual scanner, was used to take Z-stack images. The 25X Apo 1.1 NA LWD water immersion objective was used for imaging. Images were acquired with Nikon NIS elements and then converted to an .avi file format using Imaris.

In vivo GAP formation analysis with food allergens and immunofluorescence analysis in naïve and food allergic mice

Fluorescent tagged clinically relevant food allergens (cow’s milk and egg) (250μg / 200μl), model fluorescent antigens (Rh-Dex) and OVA were intraluminally injected into SI segment for 20 min to naïve mouse small intestines. In some experiments mice were injected with CCh (0.075 mg/Kg) prior to the allergen exposure. To examine how oral allergens and the imaging antigen translocate across the intestinal epithelium, naïve mice were stimulated with CCh then exposed to Rh-Dex. Allergic mouse SIs were exposed to OVA (0.45 mg/kg) and or Rh-Dex (0.0625 mg/kg) for 20 minutes prior to tissue harvest. Control group mice were injected with saline then exposed to Rh-Dex (0.0625 mg/kg). Antigen passages were quantitated by counting the frequency of antigen passages in 20 well-oriented villi per

mouse for quantitation of GAP formation. To determine the cell types translocating Rh-Dex in food allergic mice upon allergen exposure, cross sections of food allergic SIs were stained for MUC2, ChgA, MMP7 or DCLK-1. Villous and crypt antigen passing intestinal epithelial cells, $MUC2^+$ (GAP) and MUC2- (nGAP) cells in villi are quantified in 20 well oriented crypts and villi per mouse. To assess antigen passages throughout the GI tract, OVA & Rh-Dex were intraluminally injected into the stomach, ileum and colon of food allergic mice 20 min prior to tissue harvest. To examine the contribution of intestinal secretory epithelial cell antigen passages (SAP) formation during oral antigen–driven anaphylaxis, food allergy was developed in BALB/c wildtype (WT) mice as previously described [20]. The symptoms of anaphylaxis were confirmed after the 6^{th} oral antigen challenge as previously described[18]. Mice with a core body temperature loss of >1.5°C were considered positive for anaphylaxis shock response and used for antigen passage formation analysis experiment. Sixty minutes prior to the 7^{th} oral antigen challenge, food allergic mice were treated with inhibitors (either Tropicamide 0.1mg/kg 50 μL; 8-Br cADPR 0.1mg / kg 50 μL) or vehicle (50 μL saline) for a control group. Core body temperature and sign of diarrhea were monitored over 45 min after the oral antigen challenge. Mice were anesthetized, intact GI segments surgically extracted from abdominal cavity and intraluminally injected with rhodamine dextran (Rh-Dex) in 2.5 mg / 200 μL phosphate-buffered saline (PBS). SI's were harvested 20 min after the injection and fixed in 4% paraformaldehyde, sucrose-protected and embedded in OCT medium. 8-μm cross sections were cut and stained for cell markers to identify cell types and images were captured with Zeiss Apotome microscope. Antigen-passage cell numbers were quantified in at least 20 well-oriented villi per mouse to perform statistical analysis. In some experiments *Atoh1*$^{fl/fl}$*;Villin-Cre*^{ERT2} and littermate control (*Atoh1*$^{fl/fl}$*;Villin-WT*) mice and IL9Tg Atoh1^{cre*PR} IL-4Rα$^{fl/fl}$ and IL9Tg Atoh1^{WT} IL-4Rα$^{fl/fl}$ (WT) mice were intraperitoneally injected with tamoxifen (1 mg/mouse) or RU486 (200 μg/mouse) for 3 consecutive days to drive gene deletion. The mice were intravenously injected with IL-13 (0.025 μg/kg) 4 days after the initial tamoxifen or RU486 injection and SAP formation was examined as described above. To test whether IL-4 is sufficient to drive SAPs, WT BALB/c mice received rmIL-4 (65ng / 200μl i.v.) and twenty-four hours later we examined MHC II expression on splenic $B220^+$ B cells and evidence of SI SAPs as described[50]. To determine the requirement of IL-13 driven SAPs in the induction of a food-induced anaphylactic reaction, BALB/c mice that had demonstrated evidence of anaphylaxis following the fifth challenge were stratified into either isotype control or anti-IL-13Rα1 MAb treatment groups and received either isotype control Mouse IgG1 (4.5 - 5.5 μg / kg) (MOPC-21, mouse IgG1, BioXCell, Lebanon, NH) or with the anti-mouse IL13rα1 antibody (clone MS8 mouse IgG1-Kappa) (4.5 - 5.5 μg / kg) on Day 23, 25 and 27 of the experimental regime (Fig. 5). On Day 28, the mice received the 7^{th} oral OVA challenge and evidence of a food-induced anaphylactic reaction and SI SAPs were examined.

Antigen localization of mast cells in the murine food driven anaphylaxis models

Localization of Rh-Dex to MCs was assessed with immunofluorescence analysis and flow cytometric analysis. For immunofluorescence analyses, SI segments were stained for anti-mouse mast cell protease-1 (MCPT-1) (eBioscience) as described above. MCPT-1+ mast cells that colocalize with Rh-Dex were quantified under 5-10 high power fields per mouse and reported as % Rh-Dex+ mast cells of total mast cells under a high power field. For flow

cytometry analysis, mononuclear cells in lamina propria were isolated as previously described [51] and stained with PerCP-Cy5.5 conjugated antibodies against lineage markers (CD45R/B220, CD8, Ly-6G/Ly-6C, CD11c, CD3e) and with PE/Cy7 conjugated ckit, biotin conjugated ST2 followed by streptavidin conjugated APC-Cy7, and with APC conjugated FceR. Stained mononuclear cells were analyzed with a FACSCanton I (BD Biosciences). Quantitation of Rh-Dex$^+$ MCs were performed with FlowJo software (BD Bioscicence).

In vitro antigen uptake analysis, immunoblotting, and intracellular calcium measurement

The LS174T cell line was cultured as previously described [27] Cells were transduced with recombinant lentivirus carrying shRNA targeted against human *STAT6* TRC Number [0000019413] or a non-targeting control along and with polybrene at 10 μg/mL in culture medium for 36-48 h. Transduced cells were exposed to Rh-Dex (0.625 mg/ml PBS) with and without IL-13 (100 ng/ml) for 1 hr. Cells were fixed in 4% PFA for 20 min and stained for MUC2, and images were captured with Apotome. Cells were exposed to LY294002 (0, 1 and 10μM) (PI3K inhibitor) or 8-Br cADPR (0, 5 and 25μM) for 30 min prior to IL-13 stimulation and exposure to Rh-Dex. Antigen passage was quantified under a high-power field using Ziess Apotome. Six high-power field images were taken per group to perform statistical analysis. Western blot analyses were performed as previously described[25]. In brief, cell lysates harvested from controls and IL-13 (100ng/ml) for 30 min or 48 h, were loaded in 4–12% BisTris gels and transferred to a nitrocellulose membrane (Invitrogen). Total, STAT6, pSTAT6, toal AKT, pAKT^{Thr308}, actin were detected by using antibodies described in Reagents and horseradish peroxidase (HRP)-conjugated secondary antibodies. For intracellular calcium measurement, LS174T cells were pretreated with 8-Br cADPR in Krebs buffer for 30 minutes. Cells were loaded with Fluo-4 AM along with IL-13 stimulation for 30 min. Fluorescence images of Fluo-4 was acquired with an Olympus microscope with 10X objective. The fluorescent intensity from 6 representative areas was measured and normalized by subtracting an intensity of an area without cells using Slidebook software. Area under the curve (AUC) was determined by plotting the fluorescent intensity over 30 min using Prizm software.

Generation of transplanted human intestinal organoids and GAP/SAP analysis

Transplanted human intestinal organoids (tHIOs) were generated and maintained as previously described[35]. To assess GAP/SAP formation in tHIOs, NSG mice carrying tHIOs were treated with IL-13 and inhibitors (Tropicamide at 4 mg per mouse in 50 μL total volume or 8-Br cADPR at 4 μg per mouse in 50 μL) for 30 min. Rh-Dex or Alexa Fluor 647-milk was then injected in the luminal compartment of tHIOs, which was then exposed to GAP/SAP inducers (CCh at 100 μM or IL-13 at 100 ng/mL). tHIOs were fixed in 4% paraformaldehyde for 2 h at room temperature, sucrose-protected for overnight, and embedded in OCT. For immunofluorescent analysis, 8-μM thick sections were used.

Measurement of food allergy parameters

MCPT-1 level in the serum collected after the oral allergen challenge were analyzed with ELISA kit (eBioscience) as described by manufacturer. Small intestinal cross sections that were embedded in paraffin were stained with Leder stain for Chloroacetate esterase (CAE)

activity and alcian blue. Rectal temperature and hemoconcentration were measured as previously described[50].

Statistical analysis

Student t-test or one-way ANOVA, Spearman's rank coefficient correlation analysis was performed to determine statistical significance with GraphPad Prism 7 unless otherwise noted.

Supplementary Material

Refer to Web version on PubMed Central for supplementary material.

Acknowledgements

We thank members of the Divisions of Allergy and Immunology and Dr. Fred Finkelman at Cincinnati Children's Hospital Medical Center for critical review of the manuscript and insightful conversations. We would also like to thank Shawna Hottinger for editorial assistance and manuscript preparation. This work was supported by NIH R01 AI073553, R01 DK090119, P30DK078392, and U19A1070235, Department of Defense W81XWH-15-1-0517 and Food Allergy Research Education (FARE) Award (S.P.H). T.N. designed, performed, and analyzed experiments and wrote the manuscript. M.V. performed and analyzed experiments and wrote the manuscript. K.A.K., K.G.M., J.K.G., L.W., and S.V. performed and analyzed experiments. M.B., M.M., and M.H. provided crucial tools and performed experiments. R.N. and S.P.H. conceived the study, designed and analyzed experiments, and wrote the manuscript. The authors declare no competing financial interests. The data that support the findings of this study are available from the corresponding author upon request.

Funding Sources:

This work was supported by NIH DK073553, DK090119, AI112626, Food Allergy Research Education (FARE), DoD W81XWH-15-1-051730 and Food Allergy Research & Education (S.P.H.). M-FARA and Mary H. Weiser Food Allergy Center (S.P.H).

Abbreviations:

FIA	Food-induced anaphylaxis
SAP	Secretory antigen passage
GAP	goblet cell antigen passage
cADPR	cyclic Adenosine diphosphate ribose
IgE	Immunoglobulin E
TEDs	transepithelial dendrites
OVA	ovalbumin
CCh	Carbachol
HIO	human intestinal organoid
ChrA	chromogranin A
MMP7	metalloproteinase 7
2P	two photon

MC	mast cells
CCh	carbachol
Rh-Dex	rhodamine-dextran
DAPI	4’,6-diamidino-2-phenylindole
MCPT-1	mast cell protease-1
IL-13	interleukin-13
Atoh1	Atonal BHLH Transcription Factor 1
STAT6	Signal Transducer And Activator Of Transcription 6
PI3K	Phosphoinositide 3-kinase
AKT	Protein kinase B
M4AchR	muscarinic type-4 acetylcholine receptor

References

1. Sicherer SH, Sampson HA. Food allergy: Epidemiology, pathogenesis, diagnosis, and treatment. J Allergy Clin Immunol 2014; 133:291–307; quiz 8. [PubMed: 24388012]
2. Motosue MS, Bellolio MF, Van Houten HK, Shah ND, Campbell RL. Increasing Emergency Department Visits for Anaphylaxis, 2005–2014. J Allergy Clin Immunol Pract 2017; 5:171–5.e3. [PubMed: 27818135]
3. Galli SJ, Kalesnikoff J, Grimbaldeston MA, Piliponsky AM, Williams CMM, Tsai M. Mast cells as “tunable” effector and immunoregulatory cells: recent advances. Annu. Rev. Immunol. 2005; 23:749–86. [PubMed: 15771585]
4. Strait RT, Morris SC, Yang M, Qu XW, Finkelman FD. Pathways of anaphylaxis in the mouse. J Allergy Clin Immunol 2002; 109:658–68. [PubMed: 11941316]
5. Dombrowicz D, Flamand V, Brigman KK, Koller BH, Kinet JP. Abolition of anaphylaxis by targeted disruption of the high affinity immunoglobulin E receptor alpha chain gene. Cell 1993; 75:969–76. [PubMed: 8252632]
6. Lorentz A, Schwengberg S, Mierke C, Manns MP, Bischoff SC. Human intestinal mast cells produce IL-5 in vitro upon IgE receptor cross-linking and in vivo in the course of intestinal inflammatory disease. Eur J Immunol 1999; 29:1496–503. [PubMed: 10359103]
7. Santos J, Benjamin M, Yang PC, Prior T, Perdue MH. Chronic stress impairs rat growth and jejunal epithelial barrier function: role of mast cells. Am J Physiol Gastrointest Liver Physiol 2000; 278:G847–54. [PubMed: 10859213]
8. Kelefiotis D, Vakirtzi-Lemonias C. In vivo responses of mouse blood cells to platelet-activating factor (PAF): role of the mediators of anaphylaxis. Agents Actions 1993; 40:150–6. [PubMed: 8023738]
9. Strait RT, Morris SC, Smiley K, Urban JF Jr., Finkelman FD. IL-4 exacerbates anaphylaxis. J Immunol 2003; 170:3835–42. [PubMed: 12646651]
10. Sampson HA. Food allergy. Part 2: diagnosis and management. J Allergy Clin Immunol 1999; 103:981–9. [PubMed: 10359874]
11. Sampson HA. Food allergy. Part 1: immunopathogenesis and clinical disorders. J Allergy Clin Immunol 1999; 103:717–28. [PubMed: 10329801]
12. Wang J, Sampson HA. Food allergy. J Clin Invest 2011; 121:827–35. [PubMed: 21364287]
13. Galli SJ, Tsai M. IgE and mast cells in allergic disease. Nat Med 2012; 18:693–704. [PubMed: 22561833]

14. Hase K, Kawano K, Nochi T, Pontes GS, Fukuda S, Ebisawa M, et al. Uptake through glycoprotein 2 of FimH(+) bacteria by M cells initiates mucosal immune response. Nature 2009; 462:226–30. [PubMed: 19907495]
15. Neutra MR. M cells in antigen sampling in mucosal tissues. Curr Top Microbiol Immunol 1999; 236:17–32. [PubMed: 9893353]
16. Neutra MR, Frey A, Kraehenbuhl JP. Epithelial M cells: gateways for mucosal infection and immunization. Cell 1996; 86:345–8. [PubMed: 8756716]
17. Rescigno M, Urbano M, Valzasina B, Francolini M, Rotta G, Boasio R, et al. Dendritic cells express tight junction proteins and penetrate gut epithelial momlayers to sample bacteria. Nat Immunol 2001; 2:361–7. [PubMed: 11276208]
18. McDole JR, Wheeler LW, McDonald KG, Wang B, Konjufca V, Knoop KA, et al. Goblet cells deliver luminal antigen to CD103+ dendritic cells in the small intestine. Nature 2012; 483:345–9. [PubMed: 22422267]
19. Turner JR. Intestinal mucosal barrier function in health and disease. Nat Rev Immunol 2009; 9:799–809. [PubMed: 19855405]
20. Ahrens R, Osterfeld H, Wu D, Chen CY, Arumugam M, Groschwitz K, et al. Intestinal mast cell levels control severity of oral antigen-induced anaphylaxis in mice. Am J Pathol 2012; 180:1535–46. [PubMed: 22322300]
21. Osterfeld H, Ahrens R, Strait R, Finkelman FD, Renauld JC, Hogan SP. Differential roles for the IL-9/IL-9 receptor alpha-chain pathway in systemic and oral antigen-induced anaphylaxis. J Allergy Clin Immunol 2010; 125:469–76 e2. [PubMed: 20159257]
22. Forbes EE, Groschwitz K, Abonia JP, Brandt EB, Cohen E, Blanchard C, et al. IL-9— and mast cell–mediated intestinal permeability predisposes to oral antigen hypersensitivity. J Exp Med 2008; 205:897–913. [PubMed: 18378796]
23. Knoop KA, McDonald KG, McCrate S, McDole JR, Newberry RD. Microbial sensing by goblet cells controls immune surveillance of luminal antigens in the colon. Mucosal Immunol 2014.
24. Lee JB, Chen CY, Liu B, Mugge L, Angkasekwinai P, Facchinetti V, et al. IL-25 and CD4(+) TH2 cells enhance type 2 innate lymphoid cell-derived IL-13 production, which promotes IgE-mediated experimental food allergy. J Allergy Clin Immunol 2016; 137:1216–25.e5. [PubMed: 26560039]
25. Wu D, Ahrens R, Osterfeld H, Noah TK, Groschwitz K, Foster PS, et al. Interleukin-13 (IL-13)/IL-13 receptor alpha1 (IL-13Ralpha1) signaling regulates intestinal epithelial cystic fibrosis transmembrane conductance regulator channel-dependent Cl-secretion. J Biol Chem 2011; 286:13357–69. [PubMed: 21303908]
26. Shroyer NF, Helmrath MA, Wang VY, Antalffy B, Henning SJ, Zoghbi HY. Intestine-specific ablation of mouse atonal homolog 1 (Math1) reveals a role in cellular homeostasis. Gastroenterology 2007; 132:2478–88. [PubMed: 17570220]
27. Noah TK, Kazanjian A, Whitsett J, Shroyer NF. SAM pointed domain ETS factor (SPDEF) regulates terminal differentiation and maturation of intestinal goblet cells. Exp Cell Res 2010; 316:452–65. [PubMed: 19786015]
28. Deshpande DA, Dogan S, Walseth TF, Miller SM, Amrani Y, Panettieri RA, et al. Modulation of calcium signaling by interleukin-13 in human airway smooth muscle: role of CD38/cyclic adenosine diphosphate ribose pathway. Am J Respir Cell Mol Biol 2004; 31:36–42. [PubMed: 14764428]
29. Birchenough GM, Johansson ME, Gustafsson JK, Bergstrom JH, Hansson GC. New developments in goblet cell mucus secretion and function. Mucosal Immunol 2015; 8:712–9. [PubMed: 25872481]
30. Forbes EE, Groschwitz K, Abonia JP, Brandt EB, Cohen E, Blanchard C, et al. IL-9- and mast cell-mediated intestinal permeability predisposes to oral antigen hypersensitivity. J Exp Med 2008; 205:897–913. [PubMed: 18378796]
31. Wills-Karp M, Finkelman FD. Untangling the complex web of IL-4- and IL-13-mediated signaling pathways. Sci Signal 2008; 1:pe55. [PubMed: 19109238]
32. Nelms K, Keegan AD, Zamorano J, Ryan JJ, Paul WE. The IL-4 receptor: signaling mechanisms and biologic functions. Annu Rev Immunol 1999; 17:701–38. [PubMed: 10358772]

33. Hershey GK. IL-13 receptors and signaling pathways: An evolving Web. J Allergy Clin Immunol 2003; 111:677–90. [PubMed: 12704343]
34. Bitton A, Reichman H, Itan M, Karo-Atar D, Rozenberg P, Diesendruck Y, et al. A key role for IL-13 signaling via the type 2 IL-4 receptor in experimental atopic dermatitis. 2019.
35. Watson CL, Mahe MM, Munera J, Howell JC, Sundaram N, Poling HM, et al. An in vivo model of human small intestine using pluripotent stem cells. Nat Med 2014; 20:1310–4. [PubMed: 25326803]
36. Kondo M, Tamaoki J, Takeyama K, Nakata J, Nagai A. Interleukin-13 induces goblet cell differentiation in primary cell culture from Guinea pig tracheal epithelium. Am J Respir Cell Mol Biol 2002; 27:536–41. [PubMed: 12397012]
37. Stockinger S, Albers T, Duerr CU, Menard S, Putsep K, Andersson M, et al. Interleukin-13-mediated paneth cell degranulation and antimicrobial peptide release. J Innate Immun 2014; 6:530–41. [PubMed: 24556597]
38. McDermott JR, Leslie FC, D'Amato M, Thompson DG, Grencis RK, McLaughlin JT. Immune control of food intake: enteroendocrine cells are regulated by $CD4^+$ T lymphocytes during small intestinal inflammation. Gut 2006; 55:492–7. [PubMed: 16299028]
39. Abonia JP, Austen KF, Rollins BJ, Joshi SK, Flavell RA, Kuziel WA, et al. Constitutive homing of mast cell progenitors to the intestine depends on autologous expression of the chemokine receptor CXCR2. Blood 2005; 105:4308–13. [PubMed: 15705791]
40. Deshpande DA, Walseth TF, Panettieri RA, Kannan MS. CD38/cyclic ADP-ribose-mediated Ca2+ signaling contributes to airway smooth muscle hyper-responsiveness. FASEB J 2003; 17:452–4. [PubMed: 12514117]
41. Keegan AD, Nelms K, White M, Wang L, Pierce JH, Paul WE. An IL-4 receptor region containing an insulin receptor motif is important for IL-4 mediated IRS-1 phosphorylation and cell growth. Cell 1994; 76:811–20. [PubMed: 8124718]
42. Berin MC, Kiliaan AJ, Yang PC, Groot JA, Taminiau JA, Perdue MH. Rapid transepithelial antigen transport in rat jejunum: impact of sensitization and the hypersensitivity reaction. Gastroenterology 1997; 113:856–64. [PubMed: 9287977]
43. Yang PC, Berin MC, Yu LC, Conrad DH, Perdue MH. Enhanced intestinal transepithelial antigen transport in allergic rats is mediated by IgE and CD23 (FcepsilonRII). J Clin Invest 2000; 106:879–86. [PubMed: 11018076]
44. Knoop KA, Newberry RD. Goblet cells: multifaceted players in immunity at mucosal surfaces. Mucosal Immunol 2018; 11:1551–7. [PubMed: 29867079]
45. Kulkarni DH, McDonald KG, Knoop KA, Gustafsson JK, Kozlowski KM, Hunstad DA, et al. Goblet cell associated antigen passages are inhibited during Salmonella typhimur/cium infection to prevent pathogen dissemination and limit responses to dietary antigens. Mucosal Immunol 2018.
46. Knoop KA, Gustafsson JK, McDonald KG, Kulkarni DH, Coughlin PE, McCrate S, et al. Microbial antigen encounter during a preweaning interval is critical for tolerance to gut bacteria. Sci Immunol 2017; 2.
47. Lo YH, Chung E, Li Z, Wan YW, Mahe MM, Chen MS, et al. Transcriptional Regulation by ATOH1 and its Target SPDEF in the Intestine. Cell Mol Gastroenterol Hepatol 2017; 3:51–71. [PubMed: 28174757]
48. Rose MF, Ahmad KA, Thaller C, Zoghbi HY. Excitatory neurons of the proprioceptive, interoceptive, and arousal hindbrain networks share a developmental requirement for Math1. Proc Natl Acad Sci U S A 2009; 106:22462–7. [PubMed: 20080794]
49. Herbert DR, Holscher C, Mohrs M, Arendse B, Schwegmann A, Radwanska M, et al. Alternative macrophage activation is essential for survival during schistosomiasis and downmodulates T helper 1 responses and immunopathology. Immunity 2004; 20:623–35. [PubMed: 15142530]
50. Yamani A, Wu D, Waggoner L, Noah T, Koleske AJ, Finkelman F, et al. The vascular endothelial specific IL-4 receptor alpha-ABL1 kinase signaling axis regulates the severity of IgE-mediated anaphylactic reactions. J Allergy Clin Immunol 2017.
51. Chen CY, Lee JB, Liu B, Ohta S, Wang PY, Kartashov A, et al. Induction of Interleukin-9-producing Mucosal Mast cells Promotes Susceptibility to IgE-mediated Experimental Food Allergy. Immunity 2015; 43:788–802. [PubMed: 26410628]

Key Messages:

- The processes by which food allergens cross the mucosal surface and are delivered to the sub-epithelial immune compartment to promote the clinical manifestations of Food-induced anaphylaxis are largely unexplored.
- Food allergens are sampled by small intestine (SI) epithelial secretory cells (termed SAPs) that are localized to the SI villus and crypt region.
- SAPs channel food allergens to lamina propria mucosal mast cells via IL-13-CD38-cADPR-dependent process and blockade of this process inhibited the induction of clinical manifestations of FIA.
- IL-13-induced SAP sampling of food allergens was conserved in human intestinal organoids.

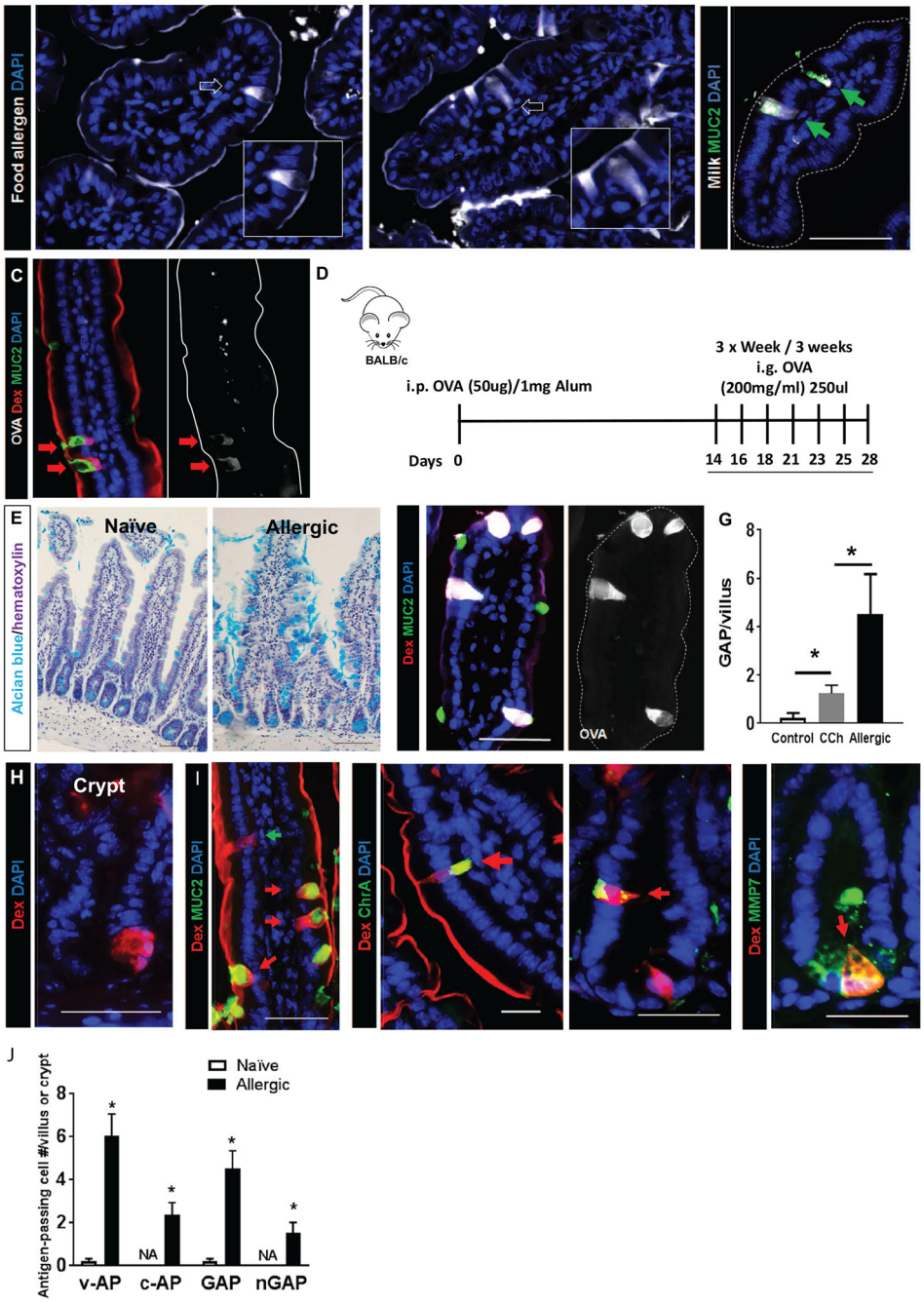

Figure 1. Antigen passage formation was dramatically increased and comprises multiple, secretory cell types in allergic mice.

(A) Immunofluorescence analysis of mouse small intestinal villus cross-sections that were exposed to milk or egg conjugated to Alexa Fluor 647 and stimulated with carbachol (CCh). White arrows point to antigen-positive intestinal epithelial cells that are morphologically identified as goblet cells shown in the insets. (B) Immunofluorescence analysis for MUC2 of mouse small intestinal villus cross-sections that were exposed to milk conjugated to Alexa Fluor 647 and stimulated with CCh. Green arrows point to MUC2+ GAPs with translocating Milk antigens. (C&F) Immunofluorescence analysis of mouse SIs from naïve, CCh-

stimulated (C) and food allergic mice that are exposed to the food antigen OVA conjugated to Alexa Fluor 647 (F, Allergic-OVA). Both mice are also exposed to the imaging antigen dextran conjugated to rhodamine (Rh-Dex; “Dex” in figure) along with the food allergen. The dotted line indicates the apical edge of the SI epithelium. (D) Diagram depicting experimental design for developing food allergy. i.p.-intraperitoneal and i.g. intragastric. (E) Alcian blue stain with hematoxylin counterstain on naïve and food allergic mouse SIs to visualize mucin-producing goblet cells. (G) GAP quantitation of naïve (saline treated control and CCh treated) and food allergic allergen challenged mouse SIs; n = 3-4 per group. Student t-test, * indicates statistical significance. (H) Immunofluorescence cross-section of SI crypt from food allergic mice. Nucleus was visualized with DAPI (blue). (I) Immunofluorescence analysis for MUC2, chromogranin A (ChrA), enteroendocrine cell marker and metalloproteinase 7 (MMP7), Paneth cell marker in allergic mice that were challenged with OVA then exposed to Rh-Dex (Dex). (J) Quantitation of antigen-positive cells, including v-AP (villus antigen-passages), c-AP (crypt antigen-passages), GAP (villous $MUC2^{+}$), and nGAP (villous $MUC2^{-}$) cells in naive, saline-treated and food allergic allergen challenged mouse SIs; n = 3-4 per group. NA denotes zero value.

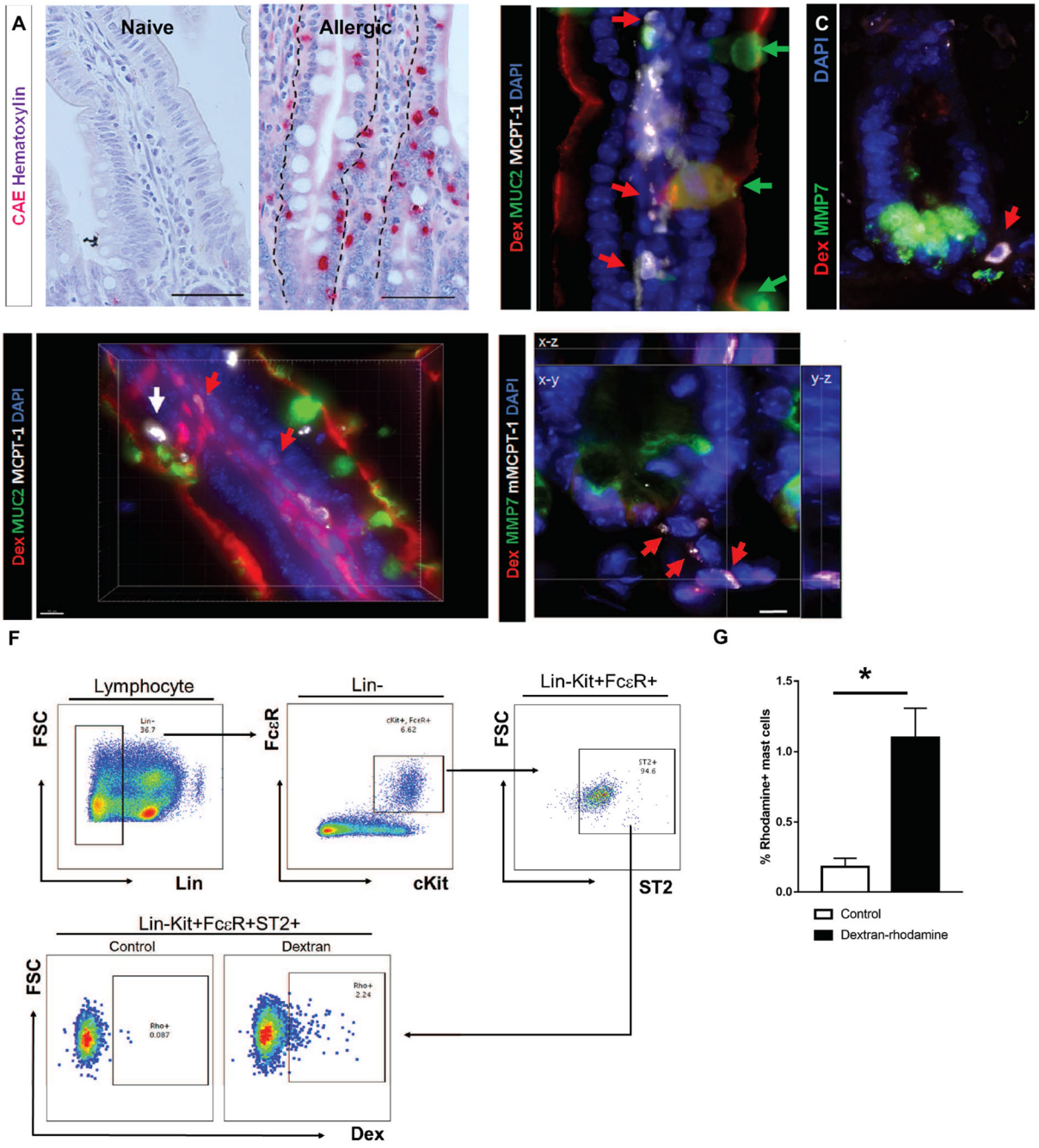

Figure 2. Antigen translocation via SAPs to underlying mast cells

(A) CAE staining with hematoxylin counterstain on naïve and allergen challenged food allergic mice. The dotted line indicates the basal edge of the SI epithelium. (B-C) Immunofluorescence analysis for (B) MUC2 (villus) or (C) MMP7 (crypt) of SIs from food allergic mice prior to the food antigen exposure; n = 3-4 mice per group. Red arrows point to mast cells residing in close proximity to goblet cells. Green arrows point to goblet cells. The dotted line indicates the basal edge of the crypt SI epithelium. (D-E) 3D reconstruction of immunofluorescence analysis for (D) MUC2 (villus) or (E) MMP7 (crypt) of SIs from food

allergic mice after the food antigen exposure; n = 3-4 mice per group. Red arrows point to Rh-Dex+ mast cells. A white arrow points to Rh-Dex^{-} intraepithelial mast cells. (F) Flow cytometry panels for gating strategies of lamina propria mast cells and the level of Rh-Dex in gated mast cells (Lin^{-}c-Kit^{+}FcεR^{+}ST2^{+}). (G) Flow cytometry analysis of mast cells in the food allergic mouse SIs for Rh-Dex. n= 8 per group. Control mice were exposed to PBS and Dextran mice were exposed to Rh-Dex along with the food allergen OVA. Data presented are the mean ± SEM. *$p < 0.05$, Student t-test or one-way ANOVA. Scale bars are 50 μm for A. Scale bars are 50, 50, 10 & 5 μm for B, C, D & F respectively. The nucleus was visualized with DAPI (blue).

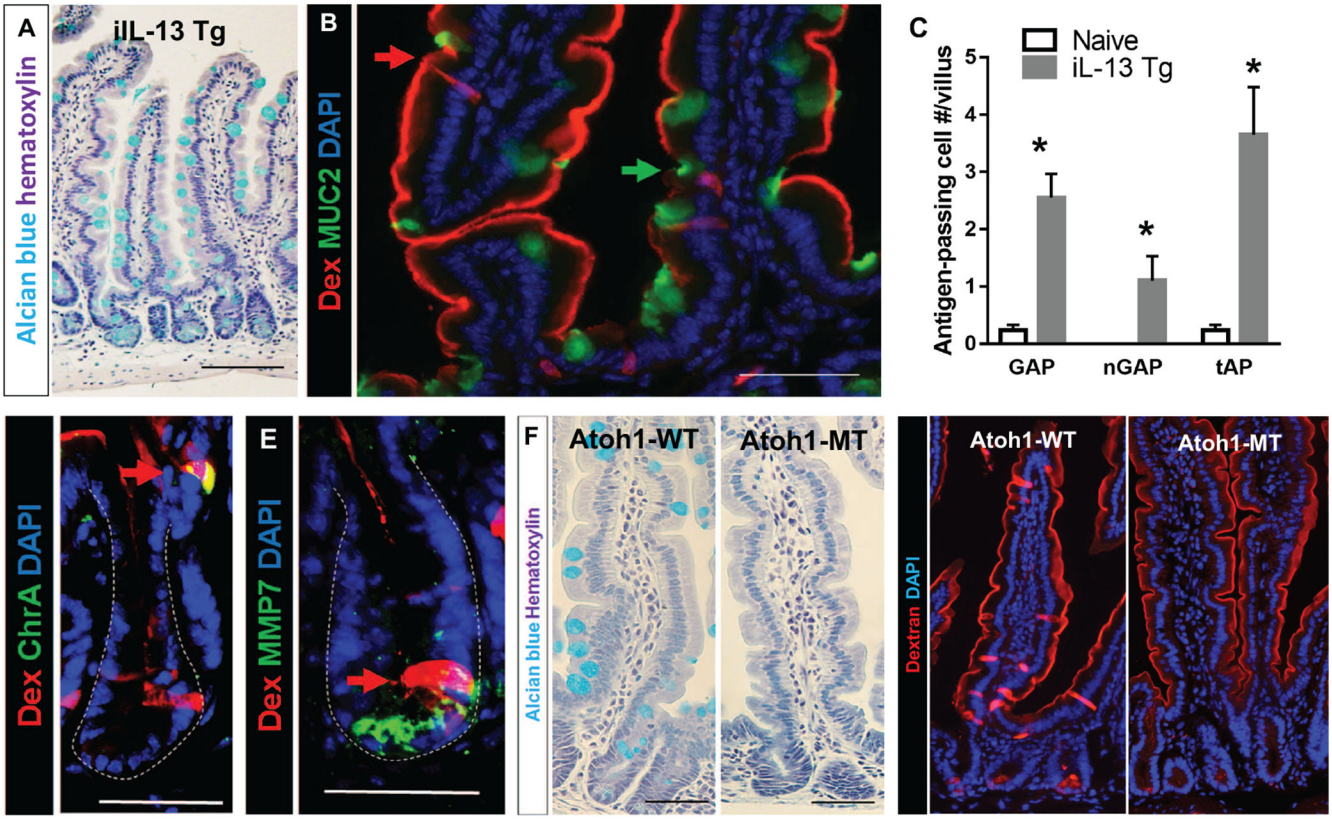

Figure 3. IL-13 is sufficient to drive SAP formation and secretory cells are required for SAP formation.

(A) Alcian blue stain with hematoxylin counterstain on ilL-13 Tg mouse SIs to visualize mucin-producing goblet cells. (B) Immunofluorescence analysis for MUC2 with iIL-13Tg mouse SI. Red arrow points to $MUC2^{-}$ antigen-passages cells, and green arrow points to $MUC2^{+}$ GAP. (C) Quantification of antigen positive cells in iIL-13 Tg and naïve control mouse SIs; n = 3-4 per group. $MUC2^{-}$ antigen positive cells are denoted as nGAP. Total antigen passages (MUC2+ and MUC2-) are denoted as tAP. (D & E) Immunofluorescence analysis for (D) ChrA, enteroendocrine cell marker or (E) MMP7, Paneth cell marker in iIL-13 Tg mouse SI crypts. Dotted lines indicate basolateral edges of crypts. (F) Alcian blue stain with hematoxylin counterstain on control (*Atoh1*-WT) and *Atohl*-deleted (*Atoh1*-MT) mouse SIs to visualize mucin-producing goblet cells. (G) Immunofluorescence analysis of control (*Atoh1*-WT) and *Atohl*-deleted (*Atoh1*-MT) SIs that were exposed to Rh-Dex. Mice were injected with IL-13 24 h prior to Rh-Dex exposure. Nucleus was visualized with DAPI. Scale bars are 50 μm.

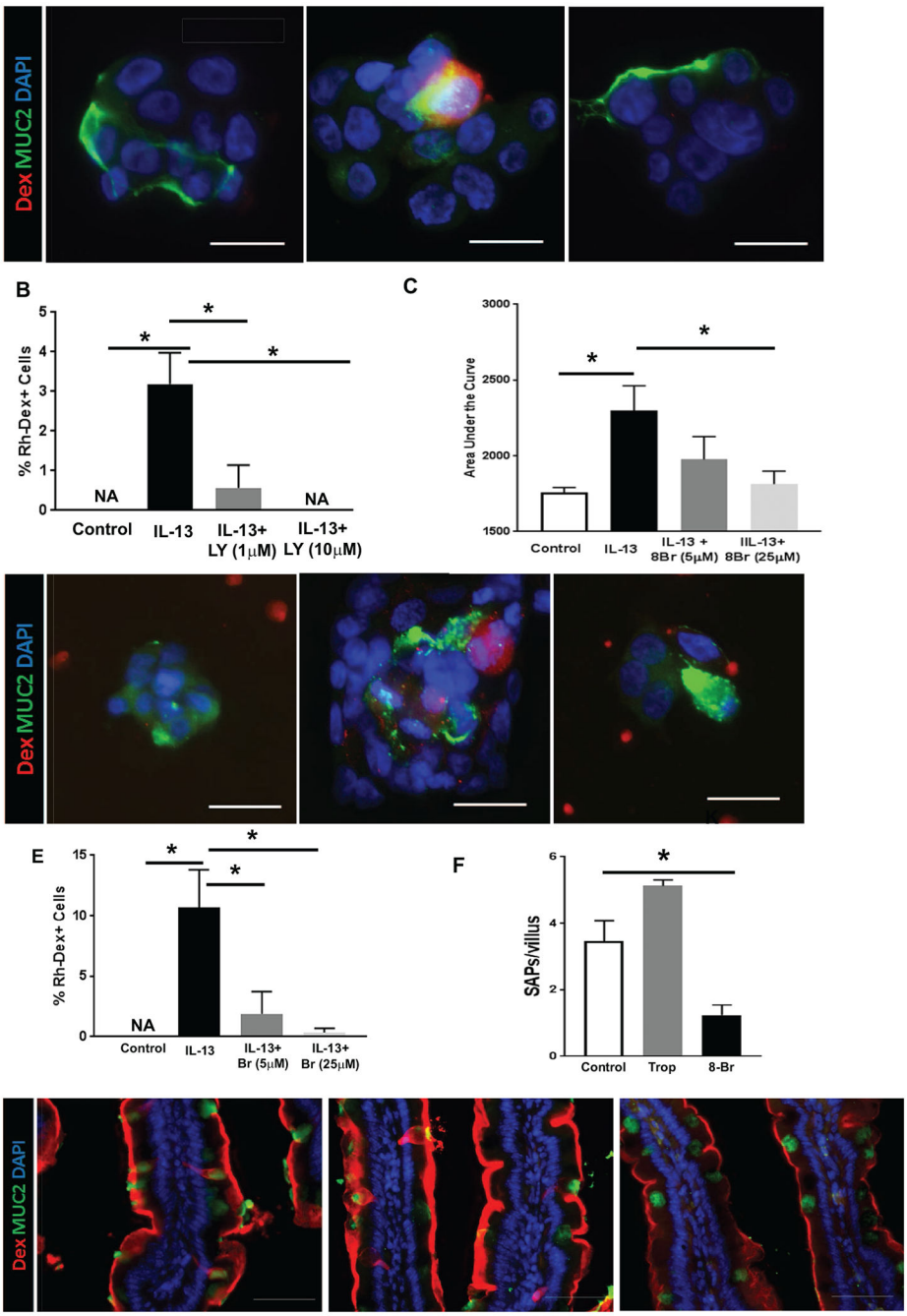

Figure 4. IL-13 drives SAP formation through the PI3K-CD38-cADPR pathway, independent of STAT6.

(A) Immunofluorescence analysis for MUC2^{+} (green) and antigen positive (red) cells treated with vehicle (Control), or PI3K inhibitor (LY294002, "LY" in figure) at 10 μM prior to IL-13 treatment and exposure to Rh-Dex (red). (B) Quantification of antigen positive cells per high-power field with cells treated as indicated in (A). (C) Intracellular calcium level measured with Furo-4 AM and quantified as area under the curve over 30 minutes (shown in supplementary Figure 2F) in cells treated with vehicle (Control), IL-13, or IL-13 and cADPR antagonist (8-Br cADPR, 8-Br in figure). (D) Immunofluorescence analysis for

MUC2^{+} (green) with cells exposed to Rh-Dex (red) and treated with vehicle (Control), or IL-13, or IL-13 and 8-Br cADPR (8-Br) at 25 μM prior to IL-13 treatment and exposure to Rh-Dex (red). (E) Quantification of antigen positive cells per high-power field with cells treated as indicated in (D). Images and cell counts are representative of three independent experiments; NA denotes zero value. (F) Quantitation of SAP formation per villus of iIL-13 Tg mouse SIs that are treated with inhibitors as indicated; Trop (Tropicamide) and 8-Br (8-Br cADPR). Twenty well-oriented villus were quantified for SAP formation; n = 3-4 mice per group. (G) Immunofluorescence analysis for SAP formation (red) and goblet cell marker, MUC2 (green), in the SIs of iIL-13 Tg mice that were treated with inhibitors as indicated; Trop (Tropicamide) and 8-Br (8-Br cADPR). (B, C, E & F) Data presented are the mean ± SEM. Scale bars are 50 μm. The nucleus was visualized with DAPI (blue). *$p < 0.05$, Student t-test or one-way ANOVA.

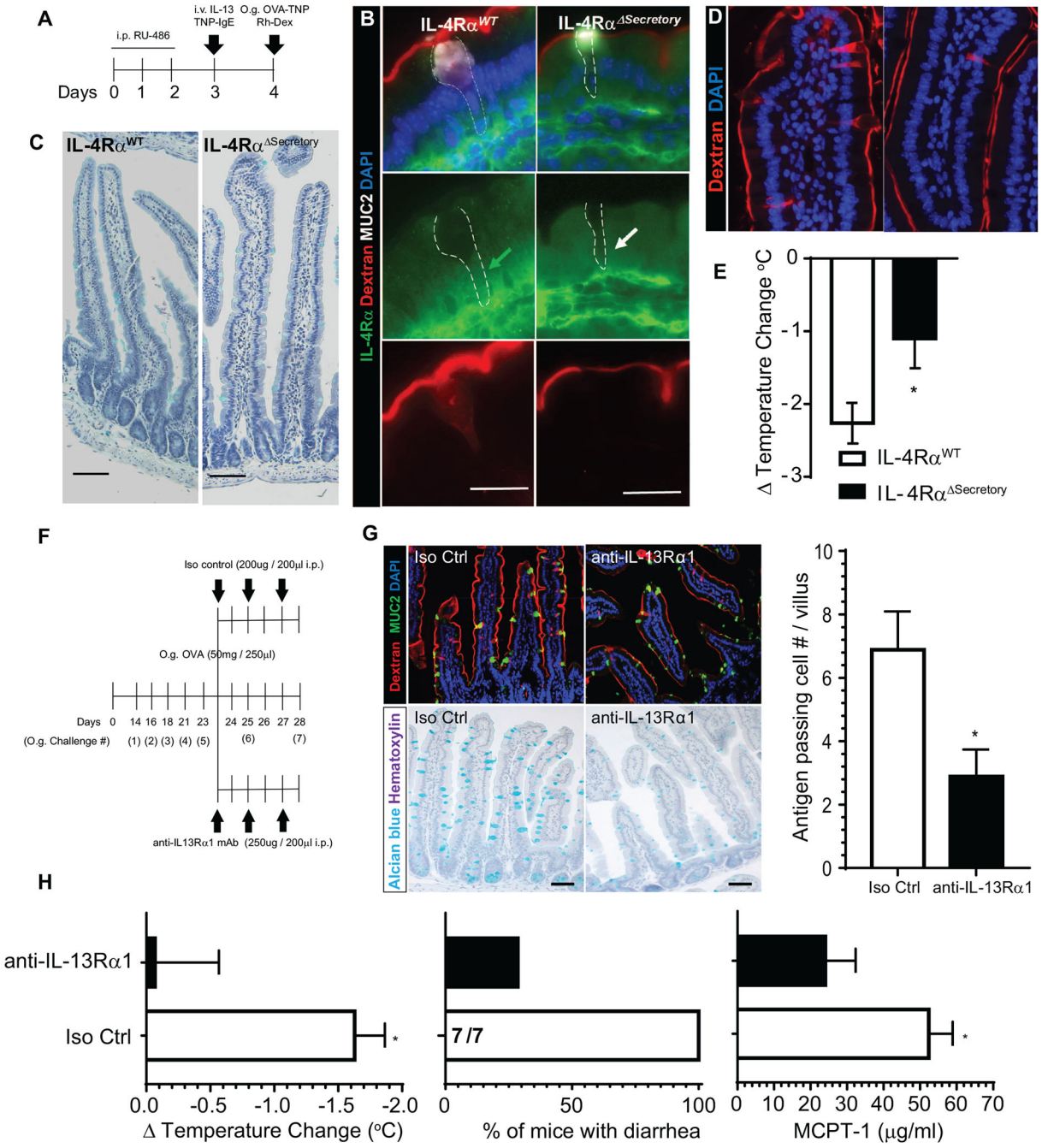

Figure 5. Type-II IL-4Rα signaling pathway is required for IL-13-induced SAP formation, luminal allergen translocation and induction of oral passive IgE- and active-food-induced anaphylaxis.

(A) Diagram depicting experimental design for inducible deletion of IL-4Rα in intestinal secretory epithelial cells. (B) Immunofluorescence analysis for IL-4Rα (green) and MUC2 (white) in mouse SIs of IL-4Rα^{WT} and IL-4Rα$^{\Delta secretory}$ mice exposed to Rh-Dex. Green arrow depicts the cytoplasm of Rh-Dex^{+} MUC2^{+} GCs in IL-4Rα^{WT} mice that are IL-4Rα^{+}. White arrow depicts cytoplasm of Rh-Dex^{+} MUC2^{+} GCs in IL-4Rα$^{\Delta secretory}$ that are IL-4Rα^{-}. The dotted line indicates GCs. (C) Alcian blue staining with hematoxylin

counterstain of SI from IL-4Rα^{WT} and IL-4Rα$^{\Delta secretory}$ mice following i.p. RU-486, (D) SI of IL9Tg IL-4Rα^{WT} and IL-9Tg IL-4Rα$^{\Delta secretory}$ mice treated with RU-486 and intraluminal SI challenge of Rh-Dex and OVA-TNP. Nucleus was visualized with DAPI and SAPs by Rh-Dex^{+} staining. (E) Δ Temperature (°C) (at 45 minutes) in IL9Tg IL-4Rα^{WT} and IL-9Tg IL-4Rα$^{\Delta secretory}$ mice treated with RU-486, IL-13 and TNP-IgE (described in A) following oral TNP-OVA challenge. *$p < 0.05$. (F) Experimental regime for neutralization of IL-13Rα1 using anti-IL-13Rα1 mAb in food allergic mice. Mice that demonstrated evidence of anaphylaxis (shock) following the 5th oral challenge were stratified into isotype control (iso control) or anti-IL-13Ra1 mAb treatment groups. Experimental analyses were performed following 7th oral challenge on Day 28. (G) Immunofluorescence analysis for MUC2 (green) and SAPs (Rh-Dex^{+}), Alcian blue staining with hematoxylin counterstain of SI and Quantitation of antigen passing cells per villus/SI from isotype control (Iso Ctrl) of SI's of control and anti-IL-13Rα1 treated mice. (H) ΔTemperature (°C), % of mice with diarrhea and serum MCPT-1 levels (at 45 minutes) in isotype control (Iso Ctrl) and anti-IL-13Rα1 treated mice following the 7th oral OVA challenge on day 28 indicated in (F). The fractions indicates the number of mice with diarrhea of the total number of mice. Scale bars are 50 μm (B, D, G, H) and 20 μm (C). i.v. intra-venous; i.p. intraperitoneal, O.g. oral gavage. * $p < 0.05$.

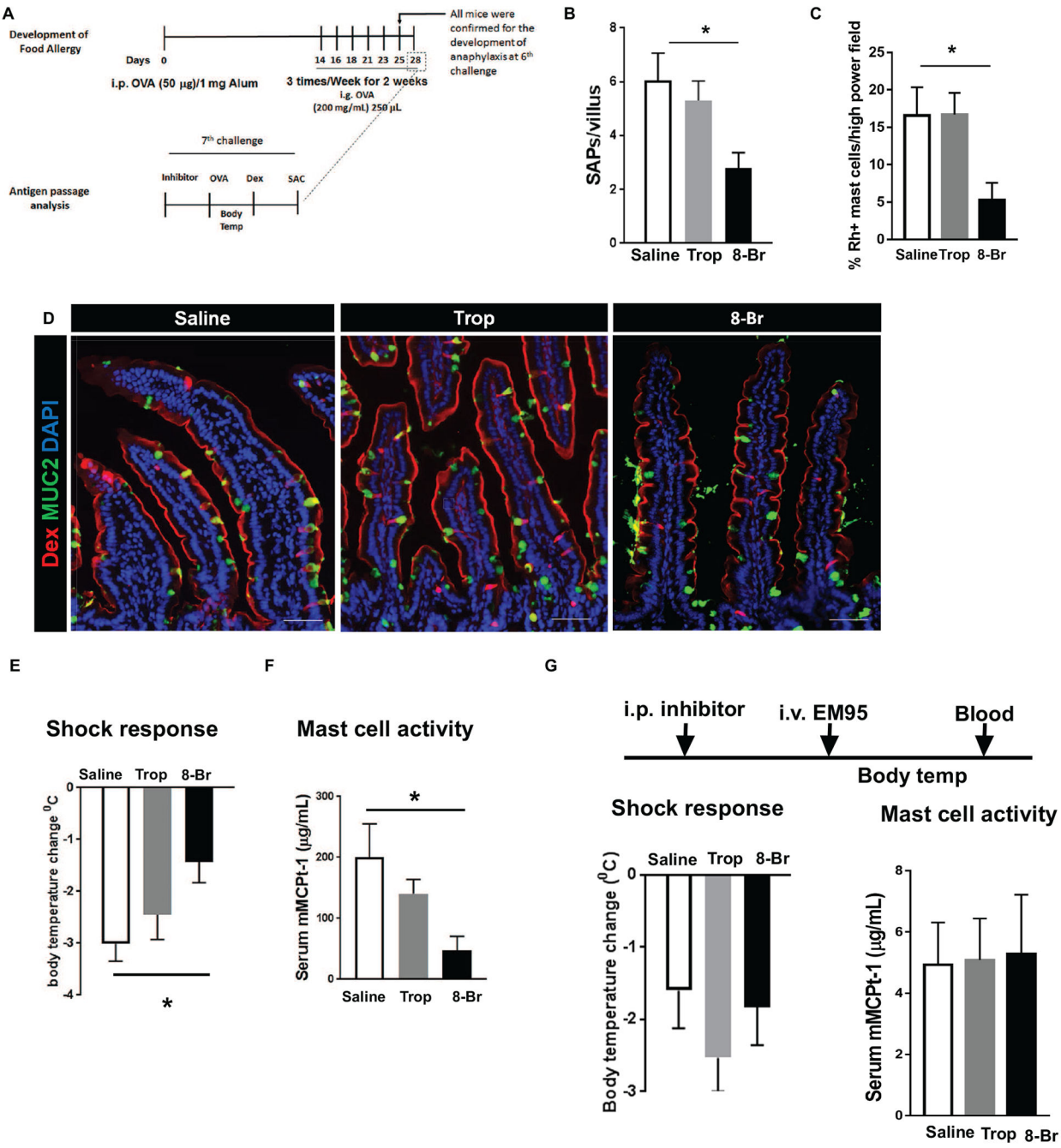

Figure 6. Blocking IL-13–driven SAP formation protects mice from the onset of acute, food-driven anaphylaxis shock.

(A) Diagram depicting experimental design for developing food allergy and analyzing SAP formation during anaphylactic shock in mice. SAC stands for sacrifice followed by tissue harvest. (B) Quantitation of SAP formation in the longitudinal SI sections of food allergic mice treated with vehicle (saline), Tropicamide (Trop), or 8-Br cADPR (8-Br). (C) Quantitation of mast cell colocalizing with dextran in SI sections of food allergic mice treated with vehicle (saline), Tropicamide (Trop), or 8-Br cADPR (8-Br). (D) Immunofluorescence analysis for MUC2 (green) and nucleus (blue) in cross sections of

allergic mouse SIs exposed to Rh-Dex after oral antigen OVA challenge. (E) Core body temperature measurement of mice after the 7th oral antigen challenge on day 28 that are treated with indicated inhibitors. (F) Serum MCPT-1 level analysis in mice treaded with indicated inhibitors. (G) Experimental design to test the effect of inhibitors on shock response driven by activating mast cells: Shock response - Core body temperature was taken after the injection of EM95 (anti-IgE antibody) as described with mice treated as indicated. Mast cell activity - Serum MCPT-1 level of mice treated as indicated after the injection of EM95. *$p < 0.05$, one-way ANOVA. n = 3-4 mice per group. Scale bars are 50 μm. Data presented are the mean ± SEM.

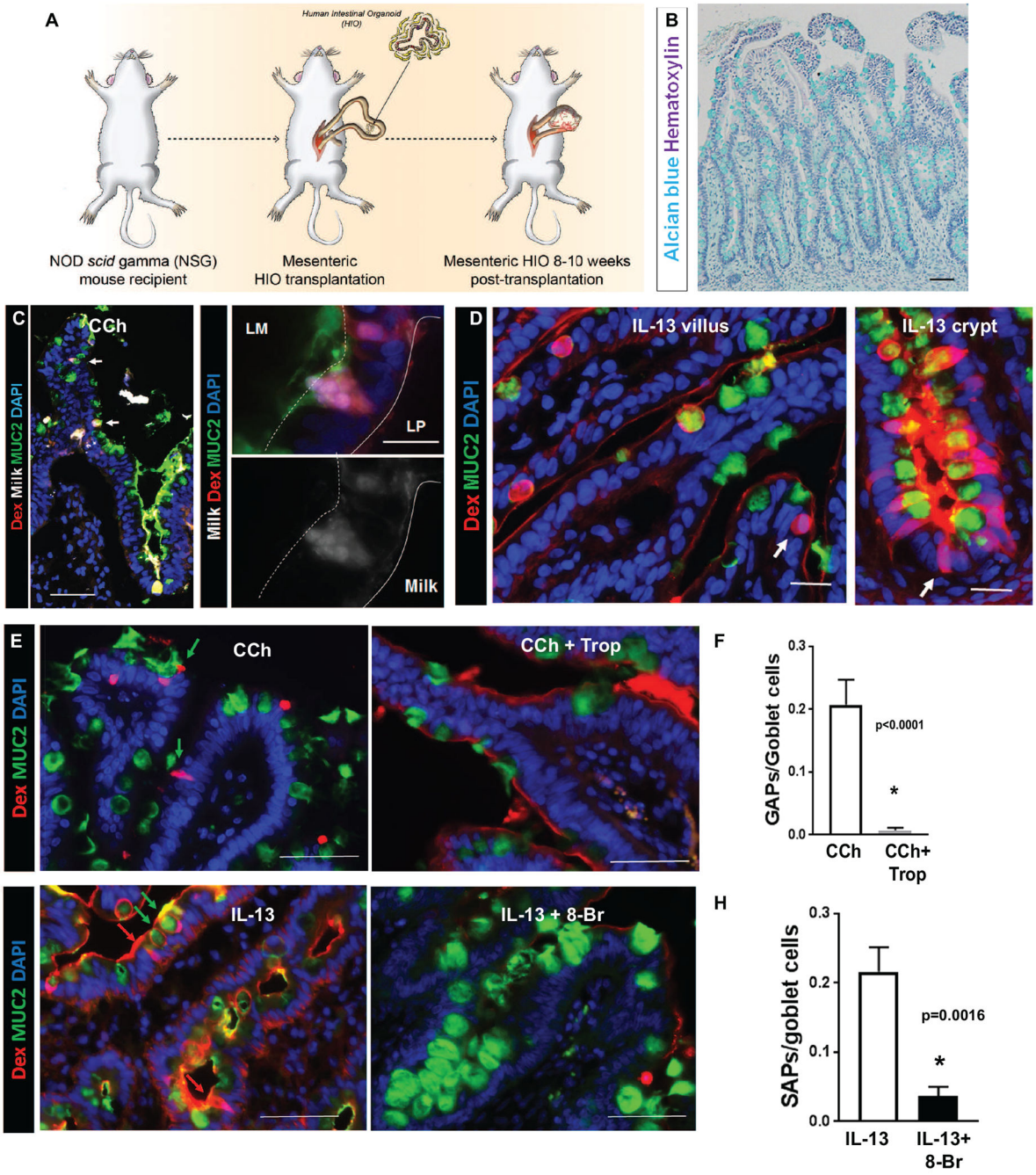

Figure 7. SAP formation pathways are conserved in human SI.

(A) Diagram of tHIO generation. (B) Alcian blue and hematoxylin of a tHIO generated as indicated in (A). (C) Immunofluorescence analysis for MUC2 (green) with in cross-sections of tHIOs exposed to Milk conjugated to Alexa 647 and Rh-Dex then stimulated with CCh. Nucleus was visualized with DAPI (blue). White arrows indicate MUC2+ Rho-Dex+ Milk-647+ GAPs. Lower (left) and higher (right) magnification images are shown. (D) Immunofluorescence analysis for MUC2 (green) with cross-sections of tHIO exposed to Rh-Dex then stimulated with IL-13. White arrows indicate MUC2^{-} antigen passages in villus

and crypts. (E&F) Immunofluorescence analysis for MUC2 (green) and nucleus (blue) of tHIOs exposed to Rh-Dex and treated as indicated. Scale bars are 50 μm. Green arrows indicate $MUC2^{+}$ Rho-Dex+ antigen passages and Red arrows indicate MUC2- Rho-Dex+ antigen passages. (F&H) Quantification of GAP (F) or SAP (H) in tHIOs. n= 3-4 per group. Student t-test. * denotes statistical significance.